

The Ecstasy and the Agony; compression studies of 3, 4-methylenedioxyamphetamine (MDMA)

Authors

Lauren E. Connor^a, Amit Delori^a, Ian B. Hutchison^a, Niamh Nic Daeid^b, Oliver B. Sutcliffe^c and Iain D.H. Oswald^{a*}

^aStrathclyde Institute of Pharmacy and Biomedical Sciences, University of Strathclyde, 161 Cathedral Street, Glasgow, G4 0RE, UK

^bCentre for Anatomy & Human Identification, University of Dundee, College of Life Sciences, Dow Street, Dundee, DD1 5EH, UK

^cSchool of Science and the Environment, Manchester Metropolitan University, Chester Street, Manchester, M1 5GD, UK

Correspondence email: iain.oswald@strath.ac.uk

Synopsis This study investigates the compression of the illicit material MDMA or “Ecstasy”.

Abstract MDMA [3,4-methylenedioxyamphetamine] is a Class A substance that is usually found in a tableted form. It is only observed in one orthorhombic polymorph under ambient conditions. It shows slight positional disorder around the methylenedioxy ring which persists during compression up to 6.66 GPa. The crystal quality deteriorates above 6.66 GPa where the hydrostatic limit of the pressure-transmitting medium is exceeded. The structure undergoes anisotropic compression with the *a*-axis compressing the greatest (12% *cf.* 4 and 10% for the *b*- and *c*-axis, respectively). This is due to the pattern of the hydrogen bonding which acts like a spring and allows the compression along this direction.

1. Introduction

3,4-Methylenedioxyamphetaminhydrochloride (MDMA) is a synthetic entactogen, which is structurally similar to methylamphetamine (MA), and acts as a CNS stimulant, producing mood enhancement, increased energy and other empathetic effects by increasing the intra-synaptic concentrations of key neurotransmitters (serotonin, dopamine and norepinephrine) (Figure 1) (Buckley, 2012, Pentney, 2001). MDMA was first synthesised (and patented) by Merck in 1912 as a potential appetite suppressant, however the company never marketed it as such. Over the next seventy years, a number of researchers evaluated the psychedelic properties of MDMA in an attempt

IMPORTANT: this document contains embedded data - to preserve data integrity, please ensure where possible that the IUCr Word tools (available from <http://journals.iucr.org/services/docxtemplate/>) are installed when editing this document.

to harness its legitimate potential in psychotherapy – with little success (Colado *et al.*, 2007). In the 1970s and 1980s, the substance surfaced on the recreational drug scene and its widespread abuse, led many countries to prohibit the possession, supply and manufacture of MDMA. Currently, in the UK, MDMA (or “*Ecstasy*”) is controlled as a Class A, Schedule 1 substance due to its illicit use as recreational drug, and its implication in a number of highly publicised fatalities (De Letter *et al.*, 2010, Turillazzi *et al.*, 2010, Verschraagen *et al.*, 2007). It is usually found in tableted form with each batch being stamped with a particular motif e.g. a Mitsubishi logo, smiley faces or letters. The tableting procedure subjects the material to elevated pressures in which conversion to other polymorphs may occur.

We have previously investigated illicit materials under high pressure conditions to investigate whether polymorphism of these materials exists (Delori *et al.*, 2014, Sathaphut *et al.*, 2014).

Pharmaceutical companies subject formulations to rigorous scrutiny to ensure that their pharmaceutical products are stable and are present in only one form under certain manufacturing conditions (do Nascimento *et al.*, 2010); this is not the case in clandestine laboratories.

Polymorphism in these materials has received little or no attention. Lee *et al.* investigated MDMA.HCl and some related compounds via ^{13}C NMR and found that there were chemical shifts induced in the racemic MDMA.HCl when mixed with lactose and suggested interaction between MDMA.HCl and lactose (Lee *et al.*, 2000). They postulated that polymorphism existed in this system however Morimoto *et al.* and Zapata-Torres *et al.* are the only groups to have investigated MDMA.HCl and the monohydrate, respectively (Morimoto *et al.*, 1998, Zapata-Torres *et al.*, 2008). The latter observation of a hydrate may have been what Lee *et al.* had detected. Nevertheless, given that polymorphism has an impact on physical properties, such as solubility and bioavailability, it could be suggested that different clandestine drug laboratories manufacture different solid-state forms of MDMA.HCl particularly in the final tableting stage. The pressure on tableting, albeit not as great as most high pressure studies (up to 600 MPa, 0.6 GPa), may convert ecstasy into different polymorphic forms as observed in many molecular complexes (Fabbiani *et al.*, 2010, Patyk *et al.*, 2012, Tumanov *et al.*, 2010, Funnell *et al.*, 2011, Millar *et al.*, 2010, Oswald & Pulham, 2008). Herein we report the compression study of ecstasy to ~ 7 GPa highlighting the structural changes that occur on compression.

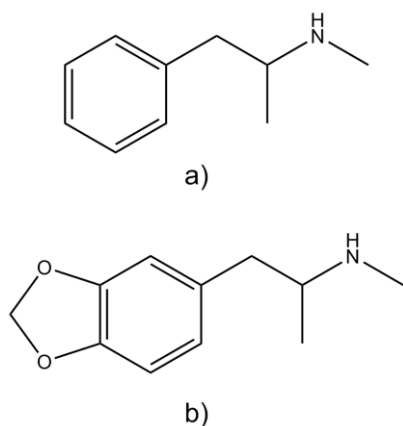


Figure 1 The chemical structures of a) MA and b) MDMA

2. Experimental

2.1. Recrystallisation

Racemic MDMA.HCl was prepared in house via the sodium borohydride method (Buchanan *et al.*, 2008), isopropyl alcohol (IPA) and petroleum ether were supplied by Sigma-Aldrich. A crude sample of MDMA.HCl was recrystallised from IPA. 20 mg (0.087 mmol) of crude MDMA.HCl was added to a vial followed by 2.5 mL of IPA. The vial was heated gently for 2 minutes before leaving the vials to return to room temperature without caps. Colourless single crystals of diffraction quality formed from this solution.

2.2. Generation of high pressure

A Merrill-Bassett Diamond anvil cell adapted to fit Boehler Almax backing discs and diamonds was used to generate the pressure in the cell (Moggach *et al.*, 2008). A tungsten foil was indented to a thickness of 100 μm and a hole (300 μm) drilled in the gasket using an Almax EasyLab Microdriller. A single crystal of MDMA.HCl, which was recrystallized from isopropanol, was loaded into the cell together with a ruby sphere (for pressure calibration) and petroleum ether which served as the pressure-transmitting medium (Piermarini *et al.*, 1975, Tateiwa & Haga, 2009). Three crystals were used to complete the high pressure datasets due to large pressure jumps between datasets in the initial compression study. Furthermore, the crystal undergoes a sharp deterioration in the diffraction above ~ 7 GPa so two further studies were made to gain a more precise pressure at which the transition occurs.

2.3. Single Crystal X-Ray Diffraction

2.3.1. Ambient pressure data collection and refinement

X-ray diffraction intensities were collected using a Bruker Apex II diffractometer with an IncoTec I μ S microsource ($\lambda=0.71073$ Å). Data were reduced using SAINT as incorporated in the APEX II suite of

programs. Absorption correction was applied using SADABS (Sheldrick, 2008). The crystal structure at ambient pressure was solved by direct methods (SIR92)(Altomare *et al.*, 1994), and refined using Crystals refinement package (Betteridge *et al.*, 2003). Distance restraints were used to ensure the geometry of the methylenedioxy ring was chemically reasonable using mean values for similar structures observed in the Cambridge Structural Database via the Mogul search.(Allen, 2002, Bruno *et al.*, 2004) The disordered model was constructed by splitting the oxygen atoms that possessed elongated thermal parameters and restraining the distances as above. The different orientations were competitively refined. Vibrational and thermal similarity restraints were applied over all atoms. The hydrogen atoms of the N1 were refined with restraints as implemented in version 14.61 of Crystals.

2.3.2. High pressure data collections and refinements

The data were collected as above but the treatment of the data was slightly modified. The data were reduced using a dynamic masking procedure as outlined in Dawson *et al.* (Dawson *et al.*, 2004). Corrections were applied using Shade (Parsons, 2004) and the absorption corrections applied using SADABS (Sheldrick, 2008). The starting point for the initial pressure was the ambient pressure model and each subsequent refinement started with the refined model from the previous pressure. Due to the low completeness of the data only the chloride ion was refined anisotropically. Similar restraints were applied to the high pressure datasets. The numbering scheme for this study is found in Figure 2 and the full crystallographic information can be found in Table 1.

Other programs used for analysis and figures were PLATON (Spek, 2003), Materials Mercury (Macrae *et al.*, 2008), OriginPro 9.0.

2.3.3. High pressure powder diffraction

The DAC was prepared as above but loaded with a powder of MDMA.HCl, a ruby and petroleum ether as the pressure transmitting medium. The cell was centred as per the single crystal experiment before a 10 minute exposure was taken. The cell was rotated by 20° during the data collection. The image was processed and the powder pattern integrated using the Pilot module within the Apex II suite of programs. A Pawley fit was performed using Topas Academic (Coelho, 2012).

2.4. Cambridge Structural database

A fragment based on the backbone of MDMA (C₇O₂) was used as a query to search the Cambridge Structural Database version 5.35 (plus all updates) via Conquest 1.16. This fragment contained no substituents and there were no restrictions applied to the search. The torsional angles around the methylenedioxy group were highlighted for retrieval. 1424 structures were found with 1952 fragments observed.

For the $\text{NH}_2^+\cdots\text{Cl}^-$ search a simple secondary ammonium group was chosen with no substituents on the neighbouring carbon atoms. Only organics with 3D coordinates determined, no polymers, errors or disorder compounds were chosen for the search.

Table 1 For all structures: $\text{C}_{11}\text{H}_{16}\text{NO}_2\cdot\text{Cl}$, orthorhombic, $Pca2_1$, $Z = 4$. Experiments were carried out at 293 K with Mo $K\alpha$ radiation using a Bruker Kappa Apex II diffractometer. Absorption was corrected for by multi-scan methods, *SADABS* (Siemens, 1996). H atoms were treated by a mixture of independent and constrained refinement. Datasets 1, 2 and 7 were collected on three different crystals however, the datasets 3-6 were collected on the same crystal.

	(1)	(2)	(3)	(4)
Crystal data				
M_r	229.71	229.71	229.71	229.71
Pressure (GPa)	Ambient	1.14	2.2	3.84
a, b, c (Å)	9.4272 (2), 7.0774 (2), 18.2519 (4)	9.1478 (3), 6.9826 (3), 17.6799 (4)	8.8661 (5), 6.9379 (4), 17.120 (3)	8.4895 (2), 6.8759 (2), 16.6225 (14)
V (Å ³)	1217.77 (3)	1129.31 (3)	1053.08 (17)	970.30 (8)
μ (mm ⁻¹)	0.30	0.32	0.34	0.37
Crystal size (mm)	0.35 × 0.22 × 0.10	0.20 × 0.10 × 0.05	0.20 × 0.10 × 0.05	0.20 × 0.10 × 0.05
Data collection				
T_{\min}, T_{\max}	0.83, 0.97	0.87, 0.98	0.87, 0.98	0.89, 0.96
No. of measured, independent and observed [$I >$ $2.0\sigma(I)$] reflections	26105, 2636, 2603	5069, 1027, 977	4833, 572, 530	4431, 522, 498
R_{int}	0.033	0.033	0.038	0.032
θ_{max} (°)	27.1	23.3	23.3	23.2
$(\sin \theta/\lambda)_{\text{max}}$ (Å ⁻¹)	0.641	0.557	0.556	0.555
Refinement				
$R[F^2 > 2\sigma(F^2)],$ $wR(F^2), S$	0.027, 0.080, 1.01	0.035, 0.081, 1.04	0.031, 0.071, 1.03	0.027, 0.062, 0.97
No. of reflections	2628	1023	567	518
No. of parameters	171	86	86	86
No. of restraints	158	56	56	56
$\Delta\rho_{\text{max}}, \Delta\rho_{\text{min}}$ (e Å ⁻³)	0.18, -0.10	0.61, -0.57	0.23, -0.22	0.14, -0.12
Absolute structure	Flack (1983), 1254 Friedel- pairs	Flack (1983), 355 Friedel-pairs	Flack (1983), 455 Friedel-pairs	Flack (1983), 50 Friedel-pairs

Absolute structure parameter	0.04 (5)	0.07 (11)	0.19 (16)	−0.02 (15)
	(5)	(6)	(7)	
Crystal data				
M_r	229.71	229.71	229.71	
Pressure (GPa)	4.42	5.24	5.98	
a, b, c (Å)	8.4043 (2), 6.8578 (2), 16.5271 (12)	8.3242 (4), 6.8403 (3), 16.447 (2)	8.3325 (8), 6.814 (2), 16.4416 (16)	
V (Å ³)	952.54 (7)	936.48 (13)	933.50 (9)	
μ (mm ^{−1})	0.38	0.38	0.39	
Crystal size (mm)	0.20 × 0.10 × 0.05	0.20 × 0.10 × 0.05	0.20 × 0.10 × 0.05	
Data collection				
T_{\min}, T_{\max}	0.91, 0.96	0.92, 0.96	0.77, 0.98	
No. of measured, independent and observed [$I > 2.0\sigma(I)$] reflections	4206, 493, 459	4137, 486, 441	2043, 510, 472	
R_{int}	0.033	0.036	0.042	
θ_{\max} (°)	23.2	23.3	23.3	
$(\sin \theta/\lambda)_{\max}$ (Å ^{−1})	0.555	0.557	0.556	
Refinement				
$R[F^2 > 2\sigma(F^2)], wR(F^2), S$	0.022, 0.055, 1.02	0.026, 0.058, 1.02	0.043, 0.106, 1.01	
No. of reflections	489	478	507	
No. of parameters	86	86	86	
No. of restraints	56	56	56	
$\Delta\rho_{\max}, \Delta\rho_{\min}$ (e Å ^{−3})	0.20, −0.22	0.22, −0.21	0.47, −0.50	
Absolute structure	Flack (1983), 29 Friedel-pairs	Flack (1983), 7 Friedel-pairs	Flack (1983), 24 Friedel-pairs	
Absolute structure parameter	0.04 (13)	−0.10 (14)	0.21 (19)	

Computer programs: Apex2 (Bruker AXS, 2006), SIR92 (Altomare *et al.*, 1994), CRYSTALS (Betteridge *et al.*, 2003)

Table 2 The hydrogen bonding parameters at each pressure

Pressure (GPa)		D-H	H...A	D...A	D-H...A
Ambient	H11-Cl1	0.914(15)	2.229(15)	3.1392(12)	173.3(15)
	H12-Cl1	0.907(15)	2.207(15)	3.0961(13)	166.7(13)
1.14	H11-Cl1	0.90(2)	2.25(2)	3.123(4)	166(2)

	H12-Cl1	0.87(2)	2.256(18)	3.072(4)	156(2)
2.2	H11-Cl1	0.91(2)	2.21(2)	3.073(4)	159(2)
	H12-Cl1	0.89(2)	2.217(18)	3.053(4)	157(2)
3.84	H11-Cl1	0.91(2)	2.20(2)	3.014(3)	150(2)
	H12-Cl1	0.874(18)	2.196(17)	3.016(4)	156(2)
4.42	H11-Cl1	0.91(2)	2.19(2)	2.998(3)	148(2)
	H12-Cl1	0.864(18)	2.198(17)	3.013(4)	157(2)
5.25	H11-Cl1	0.91(2)	2.16(2)	2.984(4)	149(2)
	H12-Cl1	0.874(18)	2.200(17)	3.009(4)	154.1(19)
5.98	H11-Cl1	0.88(2)	2.2(3)	3.003(13)	152(2)
	H12-Cl1	0.89(2)	2.19(3)	3.005(5)	153(3)

3. Results and Discussion

3.1. Ambient pressure structure

MDMA.HCl recrystallizes in one polymorphic form under ambient conditions. It crystallises in orthorhombic $Pca2_1$ with one formula unit in the asymmetric unit. We have attempted to recrystallise the sample from a range of solvents but it only had sufficient solubility in IPA and water. Crystals from IPA were of good enough quality for diffraction. The data are consistent with previous literature but we observe elongated anisotropic parameters associated with the methylenedioxy ring oxygen atoms suggesting that the ring system is disordered over two positions (Figure 2). Morimoto *et al.* did not model this disorder but the ORTEP plot from their paper also shows slightly elongated thermal parameters (Morimoto *et al.*, 1998). One factor to note is that their data collection was made at 161 K whereas the present collection was made at 293 K and so the disorder present in their structure may have been less apparent. The monohydrate structure also reveals some disordered component around one of the methylenedioxy oxygen atoms (Zapata-Torres *et al.*, 2008).

The conformation of MDMA.HCl resembles one of the lowest energy conformers around the tail group (assuming R- and S- conformations are equally low in energy)(Lee *et al.*, 2000). The angle between the least squares plane of the phenyl ring and that of the methylenedioxy group is observed to be $\sim 10^\circ$ and $\sim 27^\circ$ for the different conformations in our ambient pressure structure. These compare favourably with similar structures found in the CSD (0-25°). The rest of the molecule shows that the tail group of the cation lies almost perpendicular to the least squares plane of the ring system and that hydrogen bonds are formed between the NH_2^+ group and the Cl^- ion (N...Cl distance of 3.0961 & 3.1392 Å)(Table 2).⁶⁷ The chains of molecules are observed to run parallel to the *a*-axis with the cations lying on one side of the chain forming a cup when projected along this axis. Symmetry related chains via the 2_1 -screw axis pack closely along the *c*-axis (Figure 3). Other symmetry related chains ($1/2-x, 1+y, 1/2+z$) show close interaction between the methylene group (C70/71) with the

chloride anion and between the O10/11 and the methyl group (C11) of a neighbouring molecule ($1-x, -y, -1/2+z$).

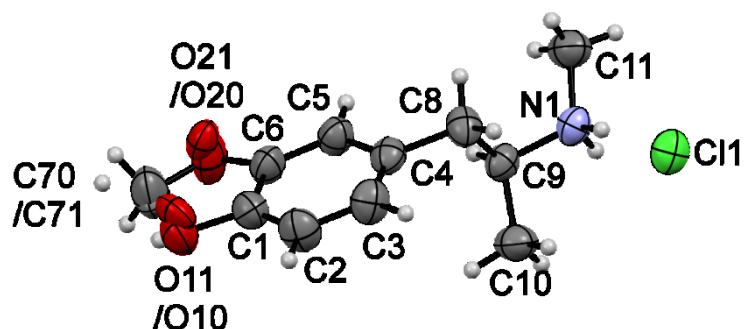


Figure 2 A displacement ellipsoid plot of MDMA.HCl at ambient pressure showing the numbering scheme used. The disordered atoms are labelled with 0 and 1 to represent the different orientations i.e. O10, C70 and O20 are one orientation and O11, C71 and O21 are the other orientation. The colour scheme for atoms is: Blue, nitrogen; grey, carbon; red, oxygen; green, chloride; white, hydrogen.

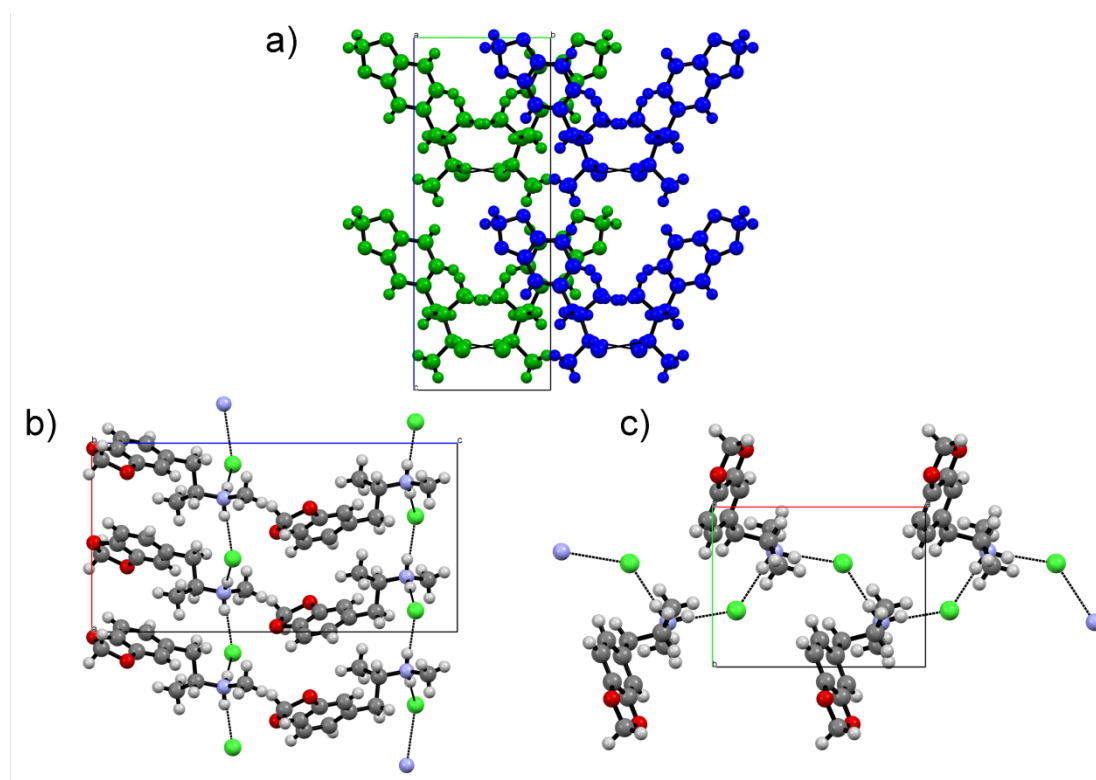


Figure 3 A view of the structure of MDMA.HCl along the a) *a*-axis (neighbouring chains along *b*-axis are coloured green and blue); b) *b*-axis; c) *c*-axis. An ordered model was used /for clarity. For 3b and 3c the colour scheme follows Figure 2 where: Blue, nitrogen; grey, carbon; red, oxygen; green, chloride; white, hydrogen.

3.2. Compression studies

The crystal structure shows a smooth anisotropic compression with the *a*-axis reducing by 12%, the *b*-axis reducing by 4% and the *c*-axis reducing by 10% up to a pressure of 6.66 GPa (Figure 4). Whilst no structural information suitable for publication could be elucidated from the data at 6.66 GPa, the unit cell parameters, space group symmetry and initial refinement shows that the ambient pressure polymorph is still present (9.28% with 232 reflections, $F^2 > 2\sigma(F^2)$).

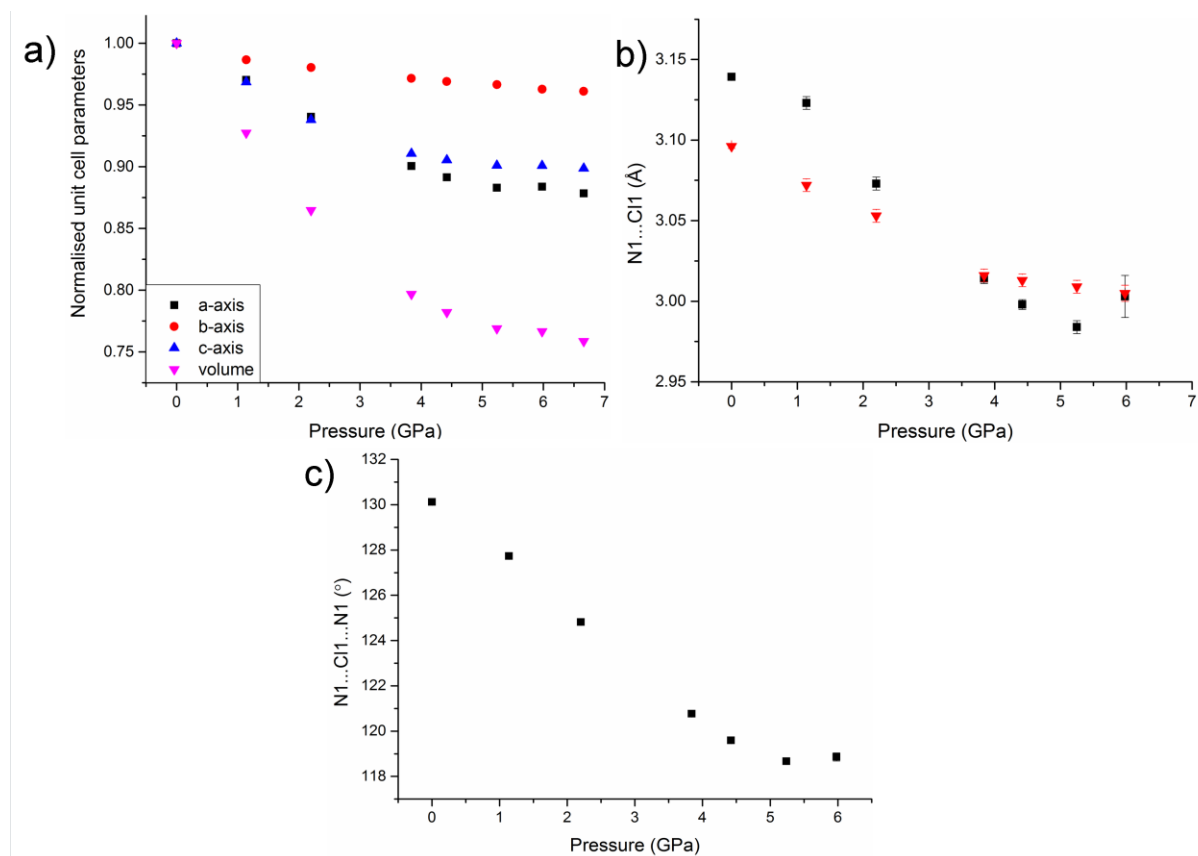


Figure 4 a) The normalised unit cell parameters and volume as a function of pressure for MDMA.HCl b) hydrogen bond lengths and c) hydrogen bonding angles as observed in MDMA.HCl as a function of pressure.

On increasing pressure the hydrogen bonding distances steadily decrease from 3.0961(13) & 3.1392(12) Å to 3.005(5) and 3.003(13) Å, respectively (Figure 4). This accounts for a 4.3% and 2.9% reduction in the hydrogen bond lengths over 5.98 GPa which is reasonable for this type of system (Figure 5). A search of the CSD shows that the hydrogen bond lengths at ambient pressure are comparable with similar types of interactions observed in a wide set of secondary ammonium complexes with chloride ions as counterions. The mean for these types of interactions is 3.126 Å from 2047 counts (837 hits) (Figure 5). On compression both of the hydrogen bonds are reduced to ~3 Å which is at the lower end of the histogram for these types of interactions; in fact one of the interactions falls below 3 Å before increasing in length again at 5.98 GPa. There are a number of compounds with extremely short bonds (CAVVUQ02 (Sysko & Allen, 1993), 2.547 Å; IWOCIH, 2.6750 Å (Wei *et al.*, 2010); XAHHAR, 2.7670 Å (Das *et al.*, 2010)) that have large molecular groups whose packing requirements need to be satisfied ahead of the hydrogen bonding; XAHHAR is an inclusion complex where the Cl⁻ is enclosed in the macrocycle.

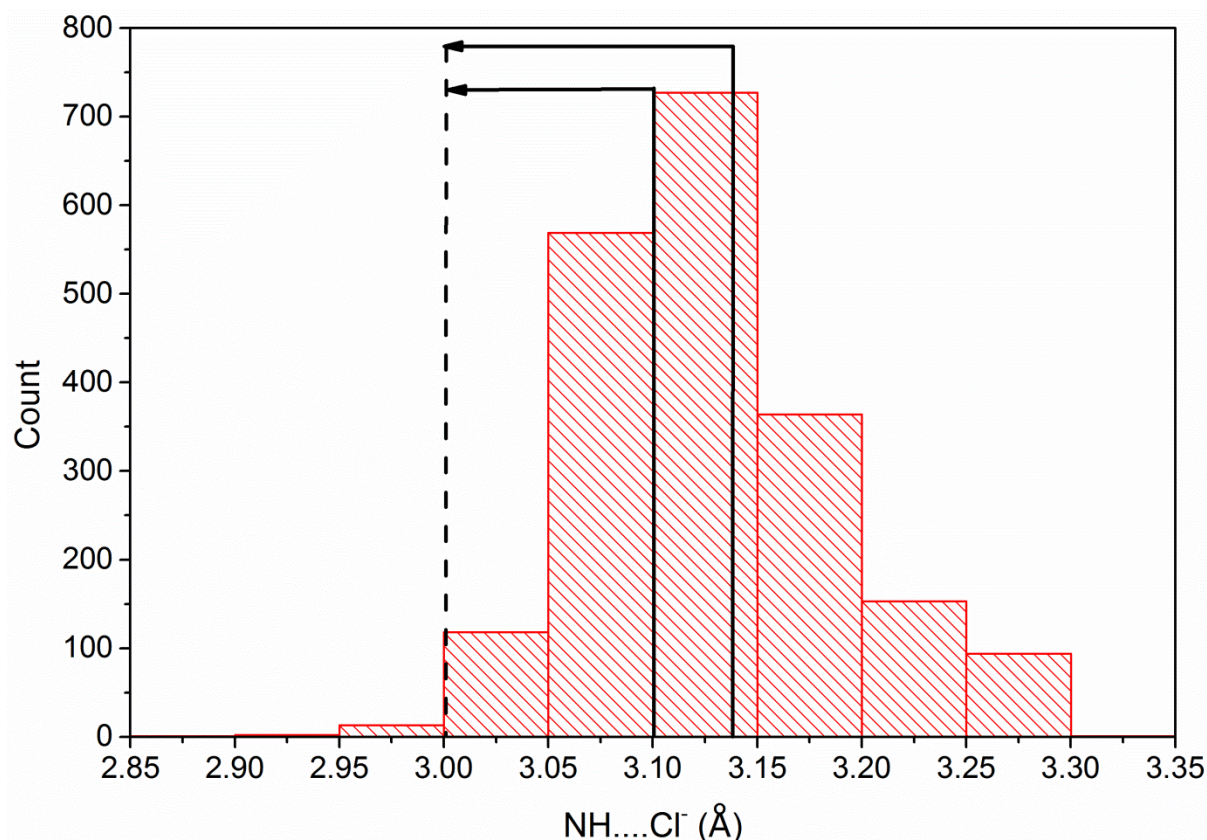


Figure 5 A histogram of $\text{NH}_2^+ \dots \text{Cl}^-$ distances observed in the CSD. The experimentally observed hydrogen bond lengths at ambient (solid) and 5.98 GPa (dotted). Compounds with hydrogen bonds shorter than 2.85 Å have been excluded for clarity of the main histogram.

Beyond 7 GPa, which is beyond the hydrostatic limit for the pressure transmitting medium, diffraction pattern deteriorates considerably (Figure 6a & b). A powder pattern of a sample at 7.27 GPa was collected on our APEX II diffractometer for 10 mins. Whilst the intensity is not particularly strong we were able to estimate the cell parameters using the previous data points and input these into Topas Academic and perform a Pawley fit on the data (Figure 6c). The fit is reasonable, considering the strength of the data, and is sufficient to conclude that the deterioration was due to the hydrostatic limit of the pressure transmitting medium and not through a reconstructive phase transition. A closer inspection of the unit cell axes shows that the compression along both the *a*- and *c*-axes have reached a minimum whilst the *b*-axis is still compressing (at 6.66 GPa) towards a minimum value. The unit cell parameters from the Pawley refinement at 7.27 GPa are $a = 8.3003$, $b = 6.7649$, $c = 16.418$ Å with a cell volume of 921.92 \AA^3 but these parameters are reported with caution. In this instance the phase remains intact but the hydrogen bond distances have compressed to a minimum suggesting that a phase transition may be imminent. Other research has highlighted that hydrogen bonds can be compressed to a minimum value as observed in the CSD before a change of phase occurs to relieve the repulsive forces (Wood *et al.*, 2008).

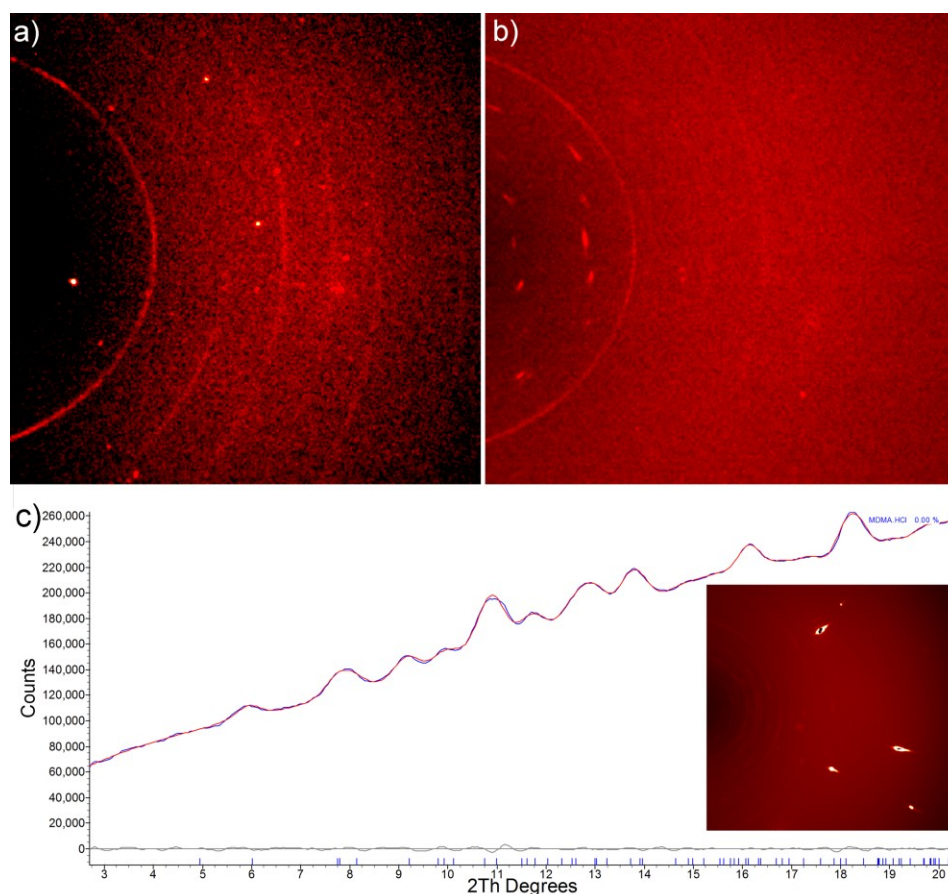


Figure 6 The diffraction patterns from the same crystal at a) 5.24 GPa, b) 7.1 GPa and c) powder at 7.27 GPa. The Pawley fit using the diffraction pattern collected on our Apex II diffractometer using the Pilot module in Apex II software.

As well as the change in the hydrogen bond distance there is a substantial alteration in the N...Cl...N angle of the hydrogen bonded chain. Figure 3c is a view perpendicular to the hydrogen bonded chain where one can observe the sinusoidal pattern of the bonding. As pressure is applied the NH...Cl distances decrease but so does the N...Cl...N angle from $\sim 130^\circ$ to 118° . One can use the analogy of a spring which is being compressed allowing for the largest compression along the *a*-axis; a more linear hydrogen bonding arrangement would not be so compressible. Void analysis of the structure shows that there are voids located in the same plane as the hydrogen bonded motif (Figure 7, circled). These voids reduce substantially on compression largely due to the compression of the hydrogen bonded chain along this direction. From the refined data, the parameters associated with the hydrogen bonding are compressed to a minimum which may signify that a phase transition may be imminent.

As described for the ambient pressure structure the hydrogen bonded chains stack along the *c*-direction. This axis is almost as compressible as the *a*-axis and this can be attributed to the lack of directional forces in this direction. Again, the voids in this direction are reduced considerably as pressure is applied. A further consequence of the compression along this direction is that, due to the

orientation of the cations with respect to the c -axis, the ‘cup’ shape as described earlier flattens which has an impact on the length of the b -axis. There have been reports of materials showing negative compressibility in wine-rack type structures under high pressure conditions. This observation is intuitive if the molecules are aligned at an angle to the principal strain axes as compression along one axis means that another is elongated (Cairns *et al.*, 2013). Whilst this structure does not show a negative compressibility it does show that the compressibility of the b -axis is significantly reduced compared with the other two axes (4% *cf.* 10 & 12% from 0 to 5.98 GPa) and this can, in part, be attributed to the molecular orientation becoming more parallel to the b -axis. Further structural features that will contribute to this are the lack of voids between neighbouring chains along the b -axis. In total the void space is reduced from 9% of the unit cell volume to 0.6%.

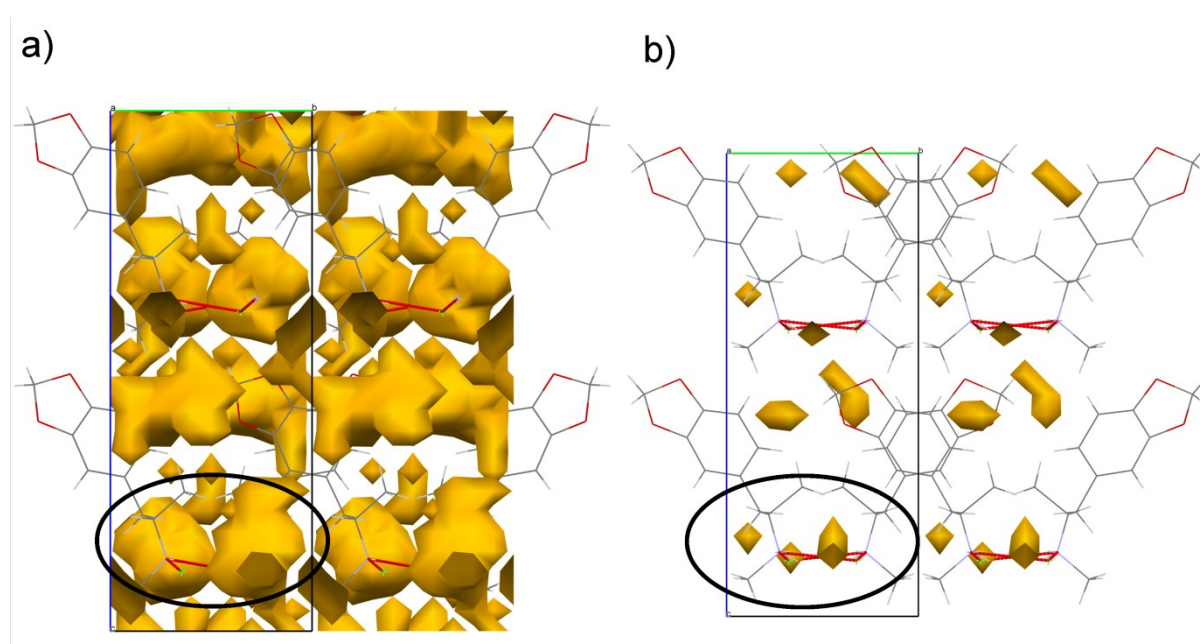


Figure 7 A view down the a -axis of the void space of MDMA.HCl at a) ambient pressure and b) 5.98 GPa calculated with Materials Mercury using a probe radius of 0.4 Å and a grid spacing of 0.7 Å. The circled area highlights the void space in one of the hydrogen bonded chains.

4. Conclusions

Despite our initial idea that polymorphism of MDMA.HCl may exist with pressure this investigation has shown that the single crystal remains in the same phase from ambient pressure to 6.66 GPa. Beyond 7 GPa the diffraction pattern deteriorates sharply which can be attributed to the hydrostatic limit of the pressure transmitting medium but the same phase is still present. The sinusoidal hydrogen bonding pattern permits the greatest compression of the structure to be along the direction of the hydrogen bonds. This is possible due to both a decrease in the bond lengths but also through the change in the N...Cl...N angle of the hydrogen bond. The orientation of the cation in the unit cell

also impacts on the rate of compressibility of the *b*-axis compared to the *a*- and *c*-axes. The compression along the *c*-axis pushes the cation towards a more parallel orientation with respect to the *b*-axis.

Acknowledgements The authors would like to acknowledge Dr Hilary Buchanan, for preparation of the MDMA and Strathclyde Institute of Pharmacy and Biomedical Sciences for funding.

References

- Allen, F. (2002). *Acta Crystallographica Section B* **58**, 380-388.
- Altomare, A., Cascarano, G., Giacovazzo, C., Guagliardi, A., Burla, M. C., Polidori, G. & Camalli, M. (1994). *Journal of Applied Crystallography* **27**, 435.
- Betteridge, P. W., Carruthers, J. R., Cooper, R. I., Prout, K. & Watkin, D. J. (2003). *Journal of Applied Crystallography* **36**, 1487.
- Bruno, I. J., Cole, J. C., Kessler, M., Luo, J., Motherwell, W. D. S., Purkis, L. H., Smith, B. R., Taylor, R., Cooper, R. I., Harris, S. E. & Orpen, A. G. (2004). *Journal of Chemical Information and Computer Sciences* **44**, 2133-2144.
- Buchanan, H. A. S., Daeid, N. N., Meier-Augenstein, W., Kemp, H. F., Kerr, W. J. & Middleditch, M. (2008). *Anal. Chem.* **80**, 3350-3356.
- Buckley, N. A. (2012). *Medical toxicology of drug abuse: Synthesized chemicals and psychoactive plants*. Hoboken, NJ: John Wiley and Sons Inc.
- Cairns, A. B., Catafesta, J., Levelut, C., Rouquette, J., van der Lee, A., Peters, L., Thompson, A. L., Dmitriev, V., Haines, J. & Goodwin, A. L. (2013). *Nat Mater* **12**, 212-216.
- Coelho, A. (2012). *Topas – academic: General profile and structure analysis software for powder diffraction data*. Version Version 5.
- Colado, I. M., O’Shea, E. & Green, R. A. (2007). *Handbook of contemporary neuropharmacology*, edited by D. R. Sibley: Wiley.
- Das, M. C., Ghosh, S. K., Sen, S. & Bharadwaj, P. K. (2010). *CrystEngComm* **12**, 2967-2974.
- Dawson, A., Allan, D. R., Parsons, S. & Ruf, M. (2004). *Journal of Applied Crystallography* **37**, 410-416.
- De Letter, E. A., Stove, C. P., Lambert, W. E. & Piette, M. H. A. (2010). *Curr. Pharm. Biotechnol.* **11**, 453-459.
- Delori, A., Maclure, P., Bhardwaj, R. M., Johnston, A., Florence, A. J., Sutcliffe, O. B. & Oswald, I. D. H. (2014). *Crystengcomm* **16**, 5827-5831.
- do Nascimento, T. G., Basilio, I. D., Macedo, R. O., Moura, E. A., Dornelas, C. B., Bernardo, V. B., Rocha, V. N. & Novak, C. (2010). *J. Therm. Anal. Calorim.* **102**, 269-275.
- Fabbiani, F. P. A., Buth, G., Dittrich, B. & Sowa, H. (2010). *Crystengcomm* **12**, 2541-2550.
- Funnell, N. P., Marshall, W. G. & Parsons, S. (2011). *CrystEngComm* **13**, 5841-5848.
- Lee, G. S. H., Taylor, R. C., Dawson, M., Kannangara, G. S. K. & Wilson, M. A. (2000). *Solid State Nucl. Magn. Reson.* **16**, 225-237.
- Macrae, C. F., Bruno, I. J., Chisholm, J. A., Edgington, P. R., McCabe, P., Pidcock, E., Rodriguez-Monge, L., Taylor, R., van de Streek, J. & Wood, P. A. (2008). *Journal of Applied Crystallography* **41**, 466-470.
- Millar, D. I. A., Oswald, I. D. H., Barry, C., Francis, D. J., Marshall, W. G., Pulham, C. R. & Cumming, A. S. (2010). *Chemical communications* **46**, 5662-5664.
- Moggach, S. A., Allan, D. R., Parsons, S. & Warren, J. E. (2008). *Journal of Applied Crystallography* **41**, 249-251.

- Morimoto, B. H., Lovell, S. & Kahr, B. (1998). *Acta Crystallogr. Sect. C-Cryst. Struct. Commun.* **54**, 229-231.
- Oswald, I. D. H. & Pulham, C. R. (2008). *Crystengcomm* **10**, 1114-1116.
- Parsons, S. (2004). *University of Edinburgh*
- Patyk, E., Skumiel, J., Podsiadlo, M. & Katrusiak, A. (2012). *Angewandte Chemie-International Edition* **51**, 2146-2150.
- Pentney, A. R. (2001). *J. Psychoact. Drugs* **33**, 213-221.
- Piermarini, G. J., Block, S., Barnett, J. D. & Forman, R. A. (1975). *J. Appl. Phys.* **46**, 2774-2780.
- Satthaphut, N., Sutcliffe, O. B. & Oswald, I. D. H. (2014). *Zeitschrift Fur Kristallographie* **229**, 101-111.
- Sheldrick, G. (2008). {sadabs (version 2008/1): Program for absorption correction for data from area detector frames}.
- Spek, A. (2003). *Journal of Applied Crystallography* **36**, 7-13.
- Sysko, R. J. & Allen, D. J. M. (1993). Hydrochloride salt, antidepressant, anorectic: Google Patents.
- Tateiwa, N. & Haga, Y. (2009). *Review of Scientific Instruments* **80**,
- Tumanov, N. A., Boldyreva, E. V., Kolesov, B. A., Kurnosov, A. V. & Cabrera, R. Q. (2010). *Acta Crystallogr. Sect. B-Struct. Sci.* **66**, 458-471.
- Turillazzi, E., Riezzo, I., Neri, M., Bello, S. & Fineschi, V. (2010). *Curr. Pharm. Biotechnol.* **11**, 500-509.
- Verschraagen, M., Maes, A., Ruiter, B., Bosman, I. J., Smink, B. E. & Lusthof, K. J. (2007). *Forensic Science International* **170**, 163-170.
- Wei, C., Rosso, V. W. & Gao, Q. (2010). Crystalline forms of (s)-7-([1,2,4]triazolo[1,5-a]pyridin-6-yl)-4-(3,4-dichlorophenyl)-1,2,3,4- tetrahydroisoquinoline and use thereof: Google Patents.
- Wood, P. A., McKinnon, J. J., Parsons, S., Pidcock, E. & Spackman, M. A. (2008). *CrystEngComm* **10**, 368-376.
- Zapata-Torres, G., Cassels, B. K., Parra-Mouchet, J., Mascarenhas, Y. P., Ellena, J. & De Araujo, A. S. (2008). *Journal of Molecular Graphics and Modelling* **26**, 1296-1305.